



APPLICATION NO. 09/826,117

INVENTION: Hybrid Walsh encoder and decoder for CDMA

INVENTORS: Urbain Alfred von der Embse

## CROSS-REFERENCE TO RELATED APPLICATIONS

### U.S. PATENT DOCUMENTS

US-6,804,307	Oct 12 2004	Popović, Branislav SE
US-6,798,737	Sept 28 2004	Dabak et. al.
US-6,674,712	Jan 6 2004	Yang et. al.
US-6,396,804	May 28 2002	Oldenwalder, Joseph P.
US-6,389,138	May 14 2002	Li et. al.
US-2002/0126,741	Sept 12 2002	Baum et. al.
US-6,317,413	Nov 13 2001	Honkasalo, Zhi-Chun
US-5,956,345	Sept 21 1999	Allpress et. al.
US-5,943,361	Aug 24 1999	Gilhousen et. al.
US-5,862,453	Jan 19 1999	Love et. al.
US-5,805,567	Sept 8 1998	Ramesh, Nallepilli S.
US-5,715,236	Feb 3 1998	Gilhousen et. al.
US-5,103,459	April 7, 1992	Gilhousen et. al.
US-5,311,176	May 10 1994	Gurney, David P.

## OTHER PUBLICATIONS

"Multiple Access for Broadband Networks", IEEE Communications magazine July 2000 Vol. 38 No. 7

"Third Generation Mobile Systems in Europe", IEEE Personal Communications April 1998 Vol. 5 No. 2

"Golay Sequences for DS CDMA Applications", J. Seberry, B.J. Wysocki and T.A. Wysocki, University of Wollongong, NSW 2522, Australia, posted on Internet

"Transmit Diversity in 3G CDMA Systems", R.T. Derryberry, S.D. Gray, D.M. Ionescu, G. Mandyam, B. Raghothaman, Nokia Research Center, 6000 Connection Drive, Irving TX 75039, posted on Internet

"Walsh functions and their Applications", K.G. Beauchamp's book, Academic Press 1975

"Discrete Complex Walsh Sequences", J. Edmund Gibbs, Div. of Electrical Science, National Physical Laboratory, Teddington, Middlesex, England, published in 1970 Report

"Application of Walsh Functions to Complex Signals", F.R. Ohnsorg, Systems and Research Div. of Honeywell, Inc. Minneapolis, Minnesota, and Office of Control Theory and Application, NASA Electronics Research Center, Cambridge, Mass., published in NRL Conference, 1970

"The Search for Hadamard Matrices", S.W. Goulomb and L.D. Baumert, Jet Propulsion Lab., Calif. Institute of Tech., published in American Math Monthly, Vol. 70, 1963

"The Z4 linearity of Kerdock, Preparata, Goethals and Related Codes", A.R. Hammons, Jr., P.V. Kumar, A.R. Calderbank, N.J.A. Sloan and P. Sole, IEEE Trans. Inform. Theory, vol. 40, pp.301-319, 1994

"Orthogonal Binary Sequences with Wide Range of Correlation Properties", B.J. Wysocki and T.A. Wysocki, School of Electrical, Computer and Telecommunications Engineering, University of Wollongong, NSW 2522, Australia, posted on the Internet

"Transmit Diversity in 3G CDMA Systems", R.T. Derryberry, S.D. Grey, D.M. Ionescu, G. Mandyam, and B. Raghothamam, Nokia Research Center, 6000 Connection Drive, Irving TX 750 75039, posted on the Internet

"Data Modulation for a Direct Sequence Pseudonoise Spread Spectrum Communication System", A.L. Kachelmyer, MIT Lincoln Lab. Project Report IFF-7, 29 Sept. 1981

"Aufbau und Eigenschaften von quasiorthogonalen Codekollektiven", W. Herold and M. Aldinger, Archiv fur Elektronik und Uebertragunstechnik, vol. 27, Nov.1973, pp. 463-470

APPLICATION NO. 09/826,117

INVENTION: Hybrid Walsh encoder and decoder for CDMA

INVENTORS: Urbain Alfred von der Embse

STATEMENT REGARDING FEDERALLY SPONSORED  
RESEARCH OR DEVELOPMENT

Not Applicable.

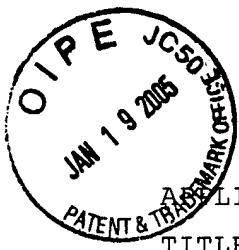
APPLICATION NO. 09/826,117

INVENTION: Hybrid Walsh encoder and decoder for CDMA

INVENTORS: Urbain Alfred von der Embse

INCORPORATION-BY-REFERENCE OF MATERIAL  
SUBMITTED ON A COMPACT DISC

Not Applicable.



APPLICATION NO.

09/826,117

TITLE OF INVENTION: Hybrid Walsh encoder and decoder for CDMA

INVENTOR: Urbain Alfred von der Embse

5

## BACKGROUND OF THE INVENTION

### 10 I. Field of the Invention

The present invention relates to CDMA (Code Division Multiple Access) cellular telephone and wireless data communications with data rates up to multiple T1 (1.544 Mbps) and higher (>100 Mbps), and to optical CDMA with data rates in the Gbps and higher ranges. Applications are mobile, point-to-point and satellite communication networks. More specifically the present invention relates to novel Hybrid Walsh codes developed to replace current real Walsh orthogonal CDMA channelization codes.

### 25 II. Description of the Related Art

CDMA art is represented by the recent work on multiple access for broadband wireless communications which includes "Multiple Access for Broadband Networks", IEEE Communications magazine July 2000 Vol. 38 No. 7, "Third Generation Mobile Systems in Europe", IEEE Personal Communications April 1998 Vol. 5 No. 2, IS-95/IS-95A, , the IS-95/IS-95A, the 3G CDMA2000 and W-CDMA, and the listed patents.

Current art using real Walsh orthogonal CDMA channelization codes considers CDMA communications spread over a common frequency band for each of the communication channels. These CDMA communications channels for each of the users are defined by assigning a unique Walsh orthogonal spreading codes to each user. The Walsh code for each user spreads the user data symbols over the common frequency band. These Walsh encoded user signals are summed and re-spread over the same frequency band by one or more PN (pseudo-noise) codes, to generate the CDMA communications signal which is modulated and transmitted. The communications link consists of a transmitter, propagation path, and receiver, as well as interfaces and control.

Transmitter Equation (1) describes a representative real Walsh CDMA encoding for the transmitter in FIG. 1A, 1B, 1C. It is assumed that there are  $N$  Walsh code vectors  $W(u)$  each of length  $N$  chips. The code vector is presented by a  $1 \times N$   $N$ -chip row vector  $W(u) = [W(u,1), \dots, W(u,N)]$  where  $W(u,n)$  is chip  $n$  of code  $u$ . The code vectors are the row vectors of the Walsh matrix  $W$ . Walsh code chip  $n$  of code vector  $u$  has the possible values  $W(u,n) = \pm 1$ . Each user is assigned a unique Walsh code which allows the code vectors to be designated by the user symbols  $u = 0, 1, \dots, N-1$  for  $N$  Walsh codes. User data symbols are the set of complex symbols  $\{Z(u), u = 0, 1, \dots, N-1\}$  and the set of equivalent real symbols  $\{R(u_R), I(u_I), u_R, u_I = 0, 1, \dots, N-1\}$  since  $Z = R + jI$  for all  $u$ , where  $j = \sqrt{-1}$  and  $u_R, u_I$  refer to different users assigned to the same real Walsh code vector  $u$ . Examples of complex user symbols are QPSK and OQPSK encoded data corresponding to 4-phase and offset 4-phase symbol coding. Examples of real user symbols are PSK and DPSK encoded data corresponding to 2-phase and differential 2-phase symbol coding.

Although not considered in this example, it is possible to use combinations of both complex and real data symbols.

## Current real Walsh CDMA encoding for transmitter **(1)**

5

### 1 Real Walsh codes

$W$  = Walsh  $N \times N$  orthogonal code matrix consisting of  
 $N$  rows of  $N$  chip code vectors  
 $= [ W(u) ]$  matrix of row vectors  $W(u)$   
 $= [ W(u,n) ]$  matrix of elements  $W(u,n)$   
 10  $W(u)$  = Walsh code vector  $u$  for  $u=0,1,\dots,N-1$   
 $= [ W(u,0), W(u,1), \dots, W(u,N-1) ]$   
 $= 1 \times N$  row vector of chips  $W(u,0), \dots, W(u,N-1)$   
 $W(u,n)$  = Walsh code  $u$  chip  $n$   
 15  $= +/ - 1$  possible values

### 2 Data symbols

$Z(u)$  = Complex data symbol for user  $u$   
 $R(u_R)$  = Real data symbol for user  $u_R$  assigned to the  
 20 Real (inphase) axis  
 $I(u_I)$  = Real data symbol for user  $u_I$  assigned to the  
 Imaginary (quadrature)

### 3 Walsh encoded data

25 Complex data symbols  
 $Z(u,n) = Z(u) \text{ sign}\{ W(u,n) \}$   
 $=$  User  $u$  chip  $n$  Walsh encoded complex data  
  
 Real components of complex data symbols  
 30  $R(u_R,n) = R(u_R) \text{ sign}\{ W(u_R,n) \}$   
 $=$  User  $u_R$  code vector  $u$  chip  $n$  Walsh encoded  
 real data  
 $I(u_I,n) = R(u_R) \text{ sign}\{ W(u_R,n) \}$   
 $=$  User  $u_I$  code vector  $u$  chip  $n$  Walsh encoded  
 35 real data



where  $\text{sign}\{ (o) \} = \text{Algebraic sign of } "(o)"$   
 $u_R$  and  $u_I$  are encoded with the same real Walsh code  
vector  $u$

5     **4** PN scrambling by long and short PN (pseudo-noise) codes

$P_2(n)$                = Chip  $n$  of PN long code

$P_R(n)$  = Chip  $n$  of PN short code for real axis  
(inphase axis)

$P_I(n)$  = Chip  $n$  of PN short code for imaginary  
10                       axis (quadrature axis)

Complex data symbols:

$Z(n)$  = PN scrambled real Walsh encoded data chips  
after summing over the users

15                       =  $\sum_u Z(u,n) P_2(n) [P_R(n) + j P_I(n)]$

=  $\sum_u Z(u,n) \text{sign}\{P_2(n)\} [\text{sign}\{P_R(n)\} + j \text{sign}\{P_I(n)\}]$

= Real Walsh CDMA encoded complex data chips

Real components of complex data symbols:

20                        $Z(n)$  =

$[\sum_{u_R} R(u_R, n) + j \sum_{u_I} I(u_I, n)] \text{sign}\{P_2(n)\} [\text{sign}\{P_R(n)\} + j \text{sign}\{P_I(n)\}]$

= Real Walsh CDMA encoded real data chips along  
inphase and quadrature axes

25

User data is encoded by the Walsh CDMA codes **3**. Each of  
the user symbols  $Z(u), R(u_R), I(u_I)$  is assigned a unique real  
Walsh code vector. Walsh encoding of each user data symbol  
30 generates an  $N$ -chip sequence with each chip in the sequence  
consisting of the user data symbol with the sign of the

corresponding Walsh code chip, which means each chip = [Data symbol] x [Sign of Walsh chip].

The Walsh encoded data symbols are summed and encoded with  
5 PN long and short spreading codes **4**. These PN long codes are real and the short codes are complex consisting of independent codes along the inphase and quadrature axes, so that the individual PN codes are 2-phase with each chip equal to  $\pm 1$  which means PN encoding consists of sign changes with each sign  
10 change corresponding to the sign of the PN chip. Encoding with PN means each chip of the summed Walsh encoded data symbols has a sign change when the corresponding PN chip is  $-1$ , and remains unchanged for  $+1$  values. This operation is described by a multiplication of each chip of the summed Walsh encoded data  
15 symbols with the sign of the PN chip.

Receiver Equation **(2)** describes a representative real Walsh CDMA decoding for the receiver in FIG. **3A, 3B**. The receiver front end **5** provides estimates  $\{\hat{Z}(n) = \hat{R}(n) + j\hat{I}(n)\}$  of the  
20 transmitted real Walsh CDMA encoded chips  $\{Z(n) = R(n) + jI(n)\}$  for the complex and real data symbols. Orthogonality property **6** is expressed as a matrix product of the real Walsh code chips or equivalently as a matrix product of the Walsh code chip numerical signs. The 2-phase PN codes **7** have the useful decoding  
25 property that the square of each code chip is unity which is equivalent to observing that the square of each code chip numerical sign is unity. Decoding algorithms **8** perform the inverse of the signal processing for the encoding in equations  
(1) to recover estimates  $\{\hat{Z}(u)\}$  or  $\{\hat{R}(u_R), \hat{I}(u_I)\}$  of the transmitter  
30 user symbols  $\{Z(u)\}$  or  $\{R(u_R), I(u_I)\}$  with  $Z(u) = R(u_R) + jI(u_I)$ .

5

5 Receiver front end provides estimates  $\{\hat{Z}(n) = \hat{R}(n) + j\hat{I}(n)\}$   
of the encoded transmitter chip symbols  $\{Z(n) = R(n) + jI(n)\}$   
for the complex and real data symbols

10

6 Orthogonality property of real Walsh NxN matrix W

$$\begin{aligned}\sum_n W(\hat{u}, n) W(n, u) &= \sum_n \text{sign}\{W(\hat{u}, n)\} \text{sign}\{W(n, u)\} \\ &= N \delta(\hat{u}, u)\end{aligned}$$

where  $\delta(\hat{u}, u)$  = Delta function of  $\hat{u}$  and u

$$= 1 \quad \text{for } \hat{u} = u$$

15

$$= 0 \quad \text{otherwise}$$

$$W' = [W(n, u)]$$

$$= \text{transpose of } W$$

7 PN decoding property

20

for real PN long code

$$\begin{aligned}P_2(n) P_2(n) &= \text{sign}\{P_2(n)\} \text{sign}\{P_2(n)\} \\ &= 1\end{aligned}$$

25

for complex PN short code

$$[P_R(n) + j P_I(n)] [P_R(n) - j P_I(n)] = 2$$

8 Decoding algorithm

30

Complex data symbols

$$\hat{Z}(u) =$$

$$N^{-1} \sum_n \hat{Z}(n) [\text{sign}\{P_2(n)\} [\text{sign}\{P_R(n)\} - j \text{sign}\{P_I(n)\}] \text{sign}\{W(n, u)\}]$$

= Receiver estimate of the transmitted complex  
data symbol  $Z(u)$

Real components of complex data symbols

$$\hat{R}(u_R) = \text{Real} \left[ N^{-1} \sum_n \hat{Z}(n) [\text{sign}\{P_R(n)\} - j \text{sign}\{P_I(n)\}] \text{sign}\{P_2(n)\} \text{sign}\{W(n, u_R)\} \right]$$

= Receiver estimate of the transmitted complex  
data symbol  $R(u_R)$

$$\hat{I}(u_I) = \text{Imag} \left[ N^{-1} \sum_n \hat{Z}(n) [\text{sign}\{P_R(n)\} - j \text{sign}\{P_I(n)\}] \text{sign}\{P_2(n)\} \text{sign}\{W(n, u_I)\} \right]$$

= Receiver estimate of the transmitted complex  
data symbol  $I(u_I)$

15

FIG. 1A CDMA transmitter block diagram is representative of a current CDMA transmitter which includes an implementation of the current real Walsh CDMA channelization encoding in equations (1). This block diagram becomes a representative implementation of the CDMA transmitter which implements the Hybrid Walsh CDMA encoding when the current real Walsh CDMA encoding 13 is replaced by the Hybrid Walsh CDMA encoding of this invention. Signal processing starts with the stream of user input data words 9. Frame processor 10 accepts these data words and performs the encoding and frame formatting, convolutional or turbo encoded, and repeated and punctured, and passes the outputs to the symbol encoder 11 which encodes the frame symbols into amplitude and phase coded symbols 12 which could be complex  $\{Z(u)\}$  or real  $\{R(u_R), I(u_I)\}$  depending on the application. These symbols 12 are the inputs to the current real Walsh CDMA encoding in equations (1). Inputs  $\{Z(u)\}, \{R(u_R), I(u_I)\}$  12 are real Walsh encoded, summed over the users, and scrambled by the real long PN code and by the complex short PN code in the current real

Walsh CDMA encoder **13** to generate the complex output chips  $\{Z(n)\}$  **14**. This encoding **13** is a representative implementation of equations **(1)**. These output chips  $Z(n)$  are waveform modulated **15** to generate the analog complex signal  $z(t)$  which is single sideband upconverted, amplified, and transmitted (Tx) by the analog front end of the transmitter **15** as the real waveform  $v(t)$  **16** at the carrier frequency  $f_0$  whose amplitude is the real part of the complex envelope of the baseband waveform  $z(t)$  multiplied by the carrier frequency and the phase angle  $\phi$  accounts for the phase change from the baseband signal to the transmitted signal.

FIG. **1B** is a representative wireless cellular communication network application of the generalized CDMA transmitter in FIG. **1A**. FIG. **1B** is a schematic layout of part of a CDMA network which depicts cells **101,102,103,104** that partition this portion of the area coverage of the network, depicts one of the users **105** located within a cell with forward and reverse communications links **106** with the cell-site base station **107**, depicts the base station communication links **108** with the MSC/WSC **109**, and depicts the MSC/WSC communication links with another base station **117**, with another MSC/WSC **116**, and with external elements **110,111,112,113,114,115**. One or more base stations are assigned to each cell or multiple cells or sectors of cells depending on the application. One of the base stations **109** in the network serves as the MSC (mobile switching center) or WSC (wireless switching center) which is the network system controller and switching and routing center that controls all of user timing, synchronization, and traffic in the network and with all external interfaces including other MSC's. External interfaces could include satellite **110**, PSTN (public switched telephone network) **111**, LAN (local area network) **112**, PAN (personal area network) **113**, UWB (ultra-wideband network) **114**, and optical networks **115**. As illustrated in the figure, base station **107** is the nominal

cell-site station for cells  $i-2$ ,  $i-1$ ,  $i$ ,  $i+1$  identified as **101,102,102,104**, which means it is intended to service these cells with overlapping coverage from other base stations. The cell topology and coverage depicted in the figure are intended to be illustrative and the actual cells could be overlapping and of differing shapes. Cells can be sub-divided into sectors. Not shown are possible subdivision of the cells into sectors and/or combining the cells into sectors. Each user in a cell or sector communicates with a base station which should be the one with the strongest signal and with available capacity. When mobile users cross over to other cells and/or are near the cell boundary a soft handover scheme is employed for CDMA in which a new cell-site base station is assigned to the user while the old cell-site base station continues to service the user for as long as required by the signal strength.

Fig. **1C** depicts a representative embodiment of the CDMA transmitter signal processing in **13,15** of FIG. **1A** for the forward and reverse CDMA links **106** in FIG. **1B** between the base station and the users for CDMA2000 and W-CDMA that implements the CDMA coding for synchronization, real Walsh channelization, and scrambling of the data for transmission. Depicted are the principal signal processing from **13,15** in FIG. **1A** that is relevant to this invention disclosure. CDMA2000 and W-CDMA use real Walsh codes **120** for channelization of the data expressed in layered format which progresses from the highest data rate for the shortest codes to the lowest data rate for the longest codes in a format referred to as OVSF (orthogonal fixed spreading factor) codes. This OVSF implementation of real Walsh codes **120** supports a variable data rate with variable length real Walsh codes over a fixed transmission channel. Long codes **122** are PN code sequences intended to provide separation of the cells and sectors and to provide protection against multipath. Long PN codes **122** for IST-95/IST-95A use code segments from a 42 bit maximal-length shift register code with code length  $(2^{42}-1)$ .

The separation between code segments is sufficient to make them statistically independent. These codes can be converted to complex codes by using the code for the real axis and a delayed version of the code for the quadrature axis. Different code  
5 segments are assigned to different cells or sectors to provide statistical independence between the communications links in different cells or sectors. Short PN codes **124,125** are used for scrambling and synchronization of CDMA code chips from the real Walsh encoding of the data symbols after they are  
10 multiplied by a long code. These codes include real and complex valued segments of maximal-length shift register sequences and segments of complex Gold codes which range in length from 256 to 38,400 chips and also are used for user separation and sector separation within a cell.

15  
FIG. **1C** data inputs **112** in FIG. **1A** to the transmitter CDMA signal processing are the inphase data symbols  $R(u_R)$  **118** and quadrature data symbols  $I(u_I)$  **119** of the complex data symbols  $Z(u) = R(u_R) + j I(u_I)$  from the block interleaving processing in the  
20 transmitter in **12** in FIG. **1A**. As described previously in Equation **(1)** in greater detail, a real Walsh code **120** ranging in length from  $N=4$  to  $N=512$  chips spreads and channelizes the data by encoding **121** the inphase and quadrature data symbols with rate  $R=N$  codes corresponding to the channel assignments of the data  
25 chips. A long PN code **122** encodes the inphase and quadrature real Walsh encoded chips **123** with a 0,1 binary code which is generated from segments of a maximal-length 42 bit shift register code for IS-95/IS-95A and an equivalent PN code for CDMA2000 and W-CDMA. Encoding is a (+/-) sign change to the chip symbols corresponding  
30 to the 0,1 code value. Long code characteristics have the PN property with quasi-orthogonal auto-correlations and cross-correlations. The long PN code **122** can be easily converted to a complex code using different code phases and families or code segments for the inphase and quadrature axes and which means in **4**  
35  $P_2(n)$  becomes complex in Equation **(1)** whereupon the encoding **123**

is replaced by a complex multiply operation similar to the short  
 code complex multiply **126** and in **4** in Equation **(1)**. This long PN  
 code covering of the real Walsh encoded chips is followed by a  
 short complex PN code covering in **124,125,126**. Short PN codes  
 5 include complex Gold code segments and complex complex valued  
 segments from maximal-length shift register codes, as well as  
 Kasami sequences, Kerdock codes, and Golay sequences. As  
 described in **4** in Equation **(1)** the complex PN short code is an  
 inphase short code **124** and a quadrature short code **125** which are  
 10 statistically independent and quasi-orthogonal. This complex PN  
 short code encodes the inphase and quadrature chips with a  
 complex multiply operation **126** as described in **4** in Equation **(1)**.  
 Outputs are inphase and quadrature components of the complex  
 chips which have been rate  $R=1$  phase coded with both the long and  
 15 short PN codes. Low pass filtering (LPF), summation ( $\Sigma$ ) over the  
 Walsh channels for each chip symbol, modulation of the chip  
 symbols to generate a digital waveform, and digital-to-analog  
 (D/A) conversion operations **127** are performed on these encoded  
 inphase and quadrature chip symbols to generate the analog  
 20 inphase  $x(t)$  signal **128** and the quadrature  $y(t)$  signal **129** which  
 are the components of the complex signal  $z(t)=x(t)+jy(t)$  where  
 $j=\sqrt{-1}$ . This complex signal  $z(t)$  is single-sideband up-converted  
 to an IF frequency and then up-converted by the RF frequency  
 front end to the RF signal  $v(t)$  **133** which is defined in **16** in  
 25 FIG. **1A**. Single sideband up-conversion of the baseband signal  
 is performed by multiplication of the inphase signal  $x(t)$  with  
 the cosine of the carrier frequency  $f_0$  **130** and the quadrature  
 signal  $y(t)$  by the sine of the carrier frequency **131** which is a  
 90 degree phase shifted version of the carrier frequency, and  
 30 summing **132** to generate the real signal  $v(t)$  **133**.

FIG. **1C** depicts an embodiment of the current CDMA  
 transmitter art and with current art signal processing changes  
 this figure is representative of other current art CDMA



transmitter embodiments for this invention disclosure. Other embodiments of the CDMA transmitter include changes in the ordering of the signal processing, single channel versus multi-channel real Walsh encoding, summation or combining of the Walsh channels by summation over like chip symbols, analog versus digital signal representation, baseband versus IF frequency CDMA processing, the order and placement in the signal processing thread of the  $\Sigma$ , LPF, and D/A signal processing operations, and the up-conversion processing. The order of the rate  $R=1$  PN multiplies in FIG. 1C can be changed since the covering operations implemented by the multiplies are linear in phase, which means the short PN code complex multiply **124,125,126** in FIG. 1C can occur prior to the long PN code multiply **122,123** and moreover the long PN code can be complex with the real multiply **123** replaced by the equivalent complex multiply **126**.

It should be obvious to anyone skilled in the communications art that this example implementation in FIG. **1A,1B,1C** clearly defines the fundamental CDMA signal processing relevant to this invention disclosure and it is obvious that this example is representative of the other possible signal processing approaches.

FIG. 2 real Walsh CDMA encoding is a representative implementation of the real Walsh CDMA encoding **13** in FIG. **1A** and **120,121** in FIG. **1C** and in equations (1). Inputs are the user data symbols which could be complex  $\{Z(u)\}$  or real ( $\{R(u_R)\}, \{I(u_I)\}$ ) **17**. For complex and real data symbols the encoding of each user by the corresponding Walsh code is described in **18** by the implementation of transferring the sign of each Walsh code chip to the user data symbol followed by a 1-to-N expander  $1 \rightarrow N$  (which is rate  $R=N$  encoding) of each data symbol into an N chip sequence using the sign transfer of the Walsh chips.

For complex data symbols  $\{Z(u)\}$  the sign-expander operation  
**18** generates the N-chip sequence  $Z(u,n) = Z(u)\text{sign}\{W(u,n)\} =$   
 $Z(u)W(u,n)$  for  $n=0,1,\dots,N-1$  for each user  $u=0,1,\dots,N-1$ . This  
Walsh encoding serves to spread each user data symbol into an  
5 orthogonally encoded chip sequence which is spread over the CDMA  
communications frequency band. The Walsh encoded chip sequences  
for each of the user data symbols are summed over the users **19**  
followed by PN encoding with the scrambling sequences  
 $P_2(n)[P_R(n)+jP_I(n)]$  **21**. PN encoding is implemented by  
10 transferring the sign of each PN chip to the summed chip of the  
Walsh encoded data symbols. Output is the stream of complex CDMA  
encoded chips  $\{Z(n)\}$  **22**. The switch **20** selects the  
appropriate signal processing path for the complex and real data  
symbols.

15 For real data symbols  $\{R(u_R)+jI(u_I)\}$  the real and imaginary  
communications axis data symbols are separately Walsh encoded  
**18**, summed **19**, and then PN encoded **21** to provide orthogonality  
between the channels along the real and imaginary communications  
20 axes. Output is the stream of complex CDMA encoded chips  $\{Z(n)\}$   
**22**.

It should be obvious to anyone skilled in the  
communications art that this example implementation in FIG. 2  
25 clearly defines the fundamental CDMA signal processing relevant  
to this invention disclosure and it is obvious that this example  
is representative of the other possible signal processing  
approaches.

30 FIG. **3A** CDMA receiver block diagram is representative of a  
current CDMA receiver which includes an implementation of the  
current real Walsh CDMA decoding in equations **(2)**. This block  
diagram becomes a representative implementation of the CDMA  
receiver which implements the Hybrid Walsh CDMA decoding when  
35 the current real Walsh CDMA decoding **27** is replaced by the

Hybrid Walsh CDMA decoding of this invention. FIG. 3A signal processing starts with the user transmitted wavefronts incident at the receiver antenna 23 for the  $n_u$  users  $u = 1, \dots, n_u \leq N_c$ . These wavefronts are combined by addition in the antenna to form the receive (Rx) signal  $\hat{v}(t)$  at the antenna output 23 where  $\hat{v}(t)$  is an estimate of the transmitted signal  $v(t)$  16 in FIG. 1A, that is received with errors in time  $\Delta t$ , frequency  $\Delta f$ , phase  $\Delta \theta$ , and with an estimate  $\hat{z}(t)$  of the transmitted complex baseband signal  $z(t)$  16 in FIG. 1A. This received signal  $\hat{v}(t)$  is amplified and downconverted by the analog front end 24 and then synchronized and analog-to-digital (ADC) converted 25. Outputs from the ADC are filtered and chip detected 26 by the fullband chip detector, to recover estimates  $\{\hat{Z}(n) = \hat{R}(n) + j\hat{I}(n)\}$  28 of the transmitted signal which is the stream of complex CDMA encoded chips  $\{Z(n) = R(n) + jI(n)\}$  14 in FIG. 1A for both complex and real data symbols. The CDMA decoder 27 implements the algorithms in equations (2) by stripping off the PN codes and decoding the received CDMA real Walsh orthogonally encoded chips to recover estimates  $\{\hat{Z}(u) = \hat{R}(u_R) + j\hat{I}(u_I)\}$  29 of the transmitted user data symbols  $\{Z(u) = R(u_R) + jI(u_I)\}$  12 in FIG. 1A. Notation introduced in FIG. 1A and 3A assumes that the user index  $u = u_R = u_I$  for complex data symbols, and for real data symbols the user index  $u$  is used for counting the user pairs  $(u_R, u_I)$  of real and complex data symbols. These estimates are processed by the symbol decoder 30 and the frame processor 31 to recover estimates 32 of the transmitted user data words.

Fig. 3B depicts a representative embodiment of the receiver signal processing 27 in FIG. 3A for the forward and reverse CDMA links 106 in FIG. 1B between the base station and the user for CDMA2000 and W-CDMA that implements the CDMA decoding for the long and short codes, the real Walsh codes, and for recovering estimates  $\hat{R}, \hat{I}$  148, 149 of the transmitted inphase and

quadrature data symbols  $R$  **118** and  $I$  **119** in FIG. **1C**. Depicted are the principal signal processing that is relevant to this invention disclosure. Signal input  $\hat{v}(t)$  **134** in FIG. **3B** is the received transmitted CDMA signal  $v(t)$  **16** in FIG. **1A** and **133** in FIG. **1C**. The signal is handed over to the inphase mixer which multiplies  $\hat{v}(t)$  by the cosine **135** of the carrier frequency  $f_0$  followed by a low pass filtering (LPF) **137** which removes the mixing harmonics, and to the quadrature mixer which multiplies  $\hat{v}(t)$  by the sine **136** of the carrier frequency  $f_0$  followed by the LPF **137** to remove the mixing harmonics. These inphase and quadrature mixers followed by the LPF perform a Hilbert transform on  $v(t)$  to down-convert the signal at frequency  $f_0$  and to recover estimates  $\hat{x}, \hat{y}$  of the inphase component  $x(t)$  and the quadrature component  $y(t)$  of the transmitted complex baseband CDMA signal  $z(t)=x(t)+jy(t)$  in **128,129** FIG. **1C**. The  $\hat{x}(t)$  and  $\hat{y}(t)$  baseband signals are analog-to-digital (D/A) **140** converted and demodulated (demod.) to recover the transmitted inphase and quadrature baseband chip symbols. The complex short PN code cover is removed by a complex multiply **143** with the complex conjugate of the short PN code implemented by using the inphase short code **141** and the negative of the quadrature short code **142** in the complex multiply operation **143**. The long PN code cover is removed by a real multiply **145** with the long code **144** implemented as  $(+/-)$  sign changes to the chip symbols since this is a binary 0,1 code. The recovered chip symbols are rate  $R=1/N$  decoded by the real Walsh decoders **146** using the real Walsh code **147** which implement the real Walsh decoding **36** in FIG. **4**. Decoded output symbols are the estimates  $\hat{R}, \hat{I}$  **148,149** of the inphase data symbols  $R$  and the quadrature data symbols  $I$  from the transmitters **12** FIG. **1A** and **118,119** FIG. **1C**.

FIG. **3B** depicts an embodiment of the current CDMA receiver art and with current art signal processing changes this figure is representative of other current art CDMA receiver embodiments for

this invention disclosure. Other embodiments of the CDMA receiver include changes in the ordering of the signal processing, analog versus digital signal representation, down-conversion processing, baseband versus IF frequency CDMA processing, order and placement in the signal processing thread of the  $\Sigma$ , LPF, and A/D signal processing operations, and single channel versus multi-channel real Walsh decoding. Code deconvolving is implemented as rate  $R=1$  code multiply operations which implement the phase subtraction of the code symbols from the chip symbols. The order of the rate  $R=N$  code multiplies in FIG. 3 can be changed since the covering operations implemented by the multiplies are linear in phase, which means the short code complex multiply **141,142,143** in FIG. 3B can occur prior to the long code multiply **144,145** and moreover the long code can be complex with the real multiply **145** replaced by the equivalent complex multiply **143**.

It should be obvious to anyone skilled in the communications art that this example implementation clearly defines the fundamental current CDMA signal processing relevant to this invention disclosure and it is obvious that this example is representative of the other possible signal processing approaches.

FIG. 4 real Walsh CDMA decoding is a representative implementation of the real Walsh CDMA decoding **27** in FIG. 3A, **144,145** in FIG. 3B, and in equations (2). Inputs are the received estimates of the complex CDMA encoded chips  $\{\hat{Z}(n)\}$  **33**. The PN scrambling code is stripped off from these chips **34** by changing the sign of each chip according to the numerical sign of the real and imaginary components of the complex conjugate of the PN code as per the decoding algorithms **8** in equations (2).

For complex data symbols **35** the real Walsh channelization coding is removed by a pulse compression operation consisting of

multiplying each received chip by the numerical sign of the corresponding Walsh chip for the user and summing the products over the N Walsh chips **36** to recover estimates  $\{\hat{Z}(u)\}$  of the user complex data symbols  $\{Z(u)\}$ . The switch **35** selects the  
5 appropriate signal processing path for the complex and real data symbols.

For real data symbols **35** the next signal processing operation is the removal of the PN codes from the real and  
10 imaginary axes. This is followed by stripping off the real Walsh channelization coding by multiplying each received chip by the numerical sign of the corresponding Walsh chip for the user and summing the products over the N Walsh chips **36** to recover estimates  $\{\hat{R}(u_R), \hat{I}(u_I)\}$  of the user real data symbols  $\{R(u_R),$   
15  $I(u_I)\}$ .

It should be obvious to anyone skilled in the communications art that this example implementation clearly defines the fundamental current CDMA signal processing relevant  
20 to this invention disclosure and it is obvious that this example is representative of the other possible signal processing approaches.

For cellular applications the transmitter description  
25 describes the transmission signal processing applicable to this invention for both the hub and user terminals, and the receiver describes the corresponding receiving signal processing for the hub and user terminals for applicability to this invention.

30 Complex Walsh codes have been proposed during the early work on Walsh bases and codes, based on the even and odd sequency property of the Walsh bases and their correspondence with the even cosine real components and odd sine imaginary components of the DFT (Discrete Fourier Transform). Sequency for

the Walsh is the average rate of phase rotations and is the Walsh equivalent of the frequency rotation for the Fourier and DFT bases. Walsh bases are re-ordered Hadamard bases where the ordering corresponds to increasing frequency. Gibbs in the 1970 report "Discrete Complex Walsh Sequences" develops a complex Walsh basis (each basis vector is a complex orthogonal CDMA code) from the real Walsh with the property that similar to the DFT the real part is an even function and the imaginary part is an odd function and takes the values  $\{1, j, -1, -j\}$  where  $j = \sqrt{-1}$ . Ohnsorg et. al. in the 1970 report "Application of Walsh Functions to Complex Signals" developed a complex Walsh basis from the real Walsh by generating a complex binary matrix from the Hadamard representation with values  $\{1, j, -1, -j\}$  and combining the scaled sum and differences of this matrix to form a complex Walsh matrix of basic vectors which gives this matrix the real even and imaginary odd properties of the DFT. These complex Walsh bases have had no apparent value in signal processing since they were not derived as an isomorphic mapping from the DFT and therefore do not exhibit any of the DFT performance advantages over the real Walsh and moreover do not have simple and fast algorithms for coding and decoding and as a result they have not been used for CDMA communications.

Golay-Hadamard sequences have been developed for CDMA which can be generated as complex sequences with values  $\{1, j, -1, -j\}$  and with a quasi-orthogonality property between basis vectors or codes. "Golay Sequences for DS (direct sequence) CDMA Applications" by Seberry et. al. and posted on the internet develops the sequences and correlation properties. These sequences are used to reduce the autocorrelation and cross-correlation sidelobes of the Hadamard and Walsh codes. Given a  $N \times N$  Hadamard matrix  $H$  or equivalently an  $N \times N$  Walsh matrix  $W$ , an  $N \times N$  diagonal matrix  $D$  can be constructed whose diagonal elements are a 2-phase (bipolar) or a 4-phase (quadri-phase) Golay

sequence of length  $N$ . For  $W$  the corresponding diagonal matrix is  $D$  which is a diagonal matrix of the same size as  $W$  and with diagonal elements consisting of a Golay sequence. With the proper selection of the Golay sequence, the sets of codes  $H \cdot D$  and  $W \cdot D$  codes have lower autocorrelation and cross-correlation sidelobes than the  $H, W$  respectively. It is observed that the autocorrelation and cross-correlation sidelobes are comparable to those obtained using a real and complex PN overlays of the  $H, W$ .

Yang (US 6,674,712) combines the quaternary complex-valued Kerdock codes with the real Walsh codes to generate a set of quasi-orthogonal CDMA codes using the complex multiply operation **126** in FIG. **1C** to combine the real Walsh codes **120**, **121** with the complex Kerdock codes upon replacing the complex short PN codes **124**, **125** with the Kerdock codes, adding a zero to the Kerdock codes of length  $(2^K - 1)$  to make them  $2^M$  chip codes and using real Walsh  $2^M$  chip codes, to allow the phase addition of these codes in the complex multiply **126**. Prior art represented by the paper by Hannon et. al. (IEEE Trans. Inform. Theory, vol. 40, pp. 301-319, 1994) and other prior publications derived the Kerdock codes with the permutation and construction algorithm in this patent. Unlike Yang, current CDMA art uses the same  $2^M$  PN code for all real Walsh channelization codes which keeps the orthogonality property while providing the desired low correlation sidelobe properties.

Li (US 6,389,138) uses the  $(2^{42} - 1)$  bit long code generator output for the inphase component and a delayed output for the quadrature component to generate a complex long code for CDMA applications. This innovation applies a code principle previously used in IS-95A,B which observes that segments of code from a maximal-length shift register code generator are statistically independent when the segments are sufficiently separated. Real Walsh codes **120** in FIG. **1C** are used for channelization codes for user traffic and communications



housekeeping functions that include pilot signals, control channels, supplemental channels, reverse channels, for both inphase and quadrature components of the complex signal **121**. With Li's invention the real Walsh inphase and quadrature encoded signals **121** are complex encoded with Li's complex long code as described in FIG. **1C** upon replacing the long PN code with Li's code and the real multiply **123** with the complex multiply **126**.

Prior art in the vol. 27 November 1973 Archive fur Elektronik und Uebertragungstechnik paper "Aufbau und Eigenschaften von quasiothogonalen Codekollektiven" and in the 1981 Lincoln Lab. report IFF-7 introduced the concept of covering the real Walsh encoded data with a real PN code in order to improve the correlation performance with time and frequency offsets. This concept was introduced well in advance of it's use in the late 1980's introduction of CDMA (US 5,103,459) wherein the real Walsh encoded data is covered by a real PN code and which covering was later updated using a complex PN code depicted in **24,25,26** FIG. **1C** and discovered in **41,42,43** FIG. **3B**.

## SUMMARY OF THE INVENTION

The present invention provides a method and system for the generation and encoding and fast decoding of Hybrid Walsh orthogonal codes for use in CDMA communications as the orthogonal channelization codes to replace the real Walsh codes. Hybrid Walsh codes are complex Walsh codes that have an isomorphic one-to-one correspondence with the DFT (discrete Fourier transform) codes. Additionally, the encoding (covering) of the Hybrid Walsh complex code by a complex PN code is a novel idea introduced in this invention disclosure.

Hybrid Walsh codes are the closest possible approximation to the DFT with orthogonal code vectors taking the values  $\{1+j, -1+j, -1-j, 1-j\}$  or equivalently the values  $\{1, j, -1, -j\}$  when the axes are rotated and renormalized where  $j=\sqrt{-1}$  and Hybrid  
5 Walsh codes offer performance improvements over real Walsh codes for CDMA communications. Hybrid Walsh codes are derived by separate lexicographic reordering permutations of real Walsh codes for the inphase (real) components and for the quadrature (imaginary) components and have simple implementations and fast  
10 encoding and decoding algorithms, where the lexicographic rule is to order the code vectors with increasing sequency. Suppression of the quadrature code components of the Hybrid Walsh codes gives the real Walsh codes along the inphase axis and suppression of the inphase code components of the Hybrid Walsh codes gives the  
15 real Walsh codes along the quadrature axis.

The invention discloses a means for the Hybrid Walsh encoder and decoder to be generalized by combining with DFT, Hadamard, and other codes using tensor product construction,  
20 direct sum construction, and functional combining. This construction increases the choices for the code length by allowing the combined use of Hybrid Walsh with lengths  $2^M$  and  $4t$  where  $M$  and  $t$  are integers, with DFT complex orthogonal codes with lengths  $N$  where  $N$  is an integer, with Hadamard codes, and  
25 with quasi-orthogonal PN families of codes including segments of maximal-length shift register codes, Gold, Kasami, Golay, Kerdock, Preparata, Goethals, STC, and with other families of codes.

30

## BRIEF DESCRIPTION OF THE DRAWINGS AND THE PERFORMANCE DATA

The above-mentioned and other features, objects, design  
5 algorithms, implementations, and performance advantages of the  
present invention will become more apparent from the detailed  
description set forth below when taken in conjunction with the  
drawings and performance data wherein like reference characters  
and numerals denote like elements, and in which:

10 FIG. **1A** is a representative CDMA transmitter signal  
processing implementation block diagram with emphasis on the  
current real Walsh CDMA encoding and which contains the signal  
processing elements addressed by this invention disclosure.

15 FIG. **1B** is a schematic CDMA cellular network with the  
communications link between a base station and a user.

20 FIG. **1C** depicts the transmit CDMA encoding signal  
processing implementation for the forward and reverse links  
between the base station and one of the users in the cellular  
network.

25 FIG. **2** is a representative CDMA encoding signal processing  
implementation diagram with emphasis on the current real Walsh  
CDMA encoding and which contains the signal processing elements  
addressed by this invention disclosure.

30 FIG. **3A** is a representative CDMA receiver signal processing  
implementation block diagram with emphasis on the current real  
Walsh CDMA decoding and which contains the signal processing  
elements addressed by this invention disclosure.

FIG. **3B** depicts the receive CDMA decoding signal processing implementation for the forward and reverse links between the base station and one of the users in the cellular network.

5

FIG. **4** is a representative CDMA decoding signal processing implementation diagram with emphasis on the current real Walsh CDMA decoding and which contains the signal processing elements addressed by this invention disclosure.

10

FIG. **5** is a representative correlation plot of the correlation between the complex discrete Fourier transform (DFT) cosine and sine code vectors and the real Fourier transform cosine and sine code vectors.

15

FIG. **6A** is a representative CDMA encoding signal processing implementation diagram with emphasis on the Hybrid Walsh CDMA encoding which contains the signal processing elements addressed by this invention disclosure

20

FIG. **6B** defines the implementation algorithm of this invention disclosure for generating Hybrid Walsh codes from real Walsh.

25

FIG. **6C** defines the implementation algorithm of this invention disclosure for generating Hybrid Walsh codes from the even and odd real Walsh codes.

30

FIG. **6D** is an embodiment of this invention disclosure for the transmit CDMA encoding signal processing implementation for the cellular network using Hybrid Walsh codes in place of real Walsh codes for the forward and reverse links between the base station and user.

FIG. **7A** is a representative CDMA decoding signal processing implementation diagram with emphasis on the Hybrid Walsh CDMA decoding and which contains the signal processing elements addressed by this invention disclosure.

5

FIG. **7B** is an embodiment of this invention disclosure for the receive CDMA decoding signal processing implementation for the cellular network using Hybrid Walsh codes in place of real Walsh codes for the forward and reverse links between the base station and user.

10

15

## DISCLOSURE OF THE INVENTION

The Hybrid Walsh complex orthogonal CDMA codes are derived from the current real Walsh codes by starting with the correspondence of the current real Walsh codes with the discrete Fourier transform (DFT) basis vectors. Consider the real orthogonal CDMA code space  $R^N$  consisting of  $N$ -orthogonal real code vectors. Examples of code sets in  $R^N$  include the Hadamard, Walsh, and Fourier. The corresponding matrices of code vectors are designated as  $H$ ,  $W$ ,  $F$  respectively and as defined in equation **(3)** respectively consist of  $N$ -rows of  $N$ -chip code vectors. Hadamard codes in their reordered form known as Walsh codes are used in the current CDMA, in the G3 CDMA, and in the proposals for all future CDMA. Walsh codes reorder the Hadamard codes according to increasing sequency which is the average rate of change of the sign of the codes. Hadamard **37** and Walsh **38** are used as code vectors for orthogonal CDMA channelization coding. Hadamard **37** and Walsh **38** equations of definition are widely known. Likewise, the Fourier **39** equations of definition are

20

25

30

35

widely known within the engineering and scientific communities,  
wherein

5 N-chip real orthogonal CDMA codes (3)

### 37 Hadamard codes

H = Hadamard NxN orthogonal code matrix consisting of  
N rows of N chip code vectors  
10 = [ H(u) ] matrix of row vectors H(u)  
= [ H(u,n) ] matrix of elements H(u,n)  
H(u) = Hadamard code vector u  
= [ H(u,0), H(u,1), ..., H(u,N-1) ]  
= 1xN row vector of chips H(u,0),...,H(u,N-1)  
15 H(u,n) = Hadamard code u chip n  
= +/-1 possible values  
=  $(-1)^{\sum_{i=0}^{M-1} u_i n_i}$   
where  $u = \sum_{i=0}^{M-1} u_i 2^i$  binary representation of u  
 $n = \sum_{i=0}^{M-1} n_i 2^i$  binary representation of n

20

### 38 Walsh codes

W = Walsh NxN orthogonal code matrix consisting of  
N rows of N chip code vectors  
= [ W(u) ] matrix of row vectors W(u)  
25 = [ W(u,n) ] matrix of elements W(u,n)  
W(u) = Walsh code vector u  
= [ W(u,0), W(u,1), ..., W(u,N-1) ]  
W(u,n) = Walsh code u chip n  
= +/-1 possible values  
30 =  $(-1)^{u_{M-1} n_0 + \sum_{i=1}^{M-1} (u_{M-1-i} + u_{M-i}) n_i}$

### 39 Fourier codes

F = Fourier NxN orthogonal code matrix consisting of  
N rows of N chip code vectors

$$\begin{aligned} &= [ F(u) ] \text{ matrix of row vectors } F(u) \\ &= \begin{bmatrix} C \\ S \end{bmatrix} \end{aligned}$$

C = N/2+1 x N matrix of row vectors C(u)

C(u) = Even code vectors for u=0,1,...,N/2

$$= [1, \cos(2\pi u/2N), \dots, \cos(2\pi u(N-1)/2N)]$$

10 S = N/2-1 x N matrix of row vectors S(u)

S(Δu) = Odd code vectors for u=N/2+Δu, Δu=1,2,...,N/2-1

$$= [\sin(2\pi \Delta u/2N), \dots, \sin(2\pi \Delta u(N-1)/2N)]$$

where F(u) = C(u) for u=0,1,...,N/2

$$= S(\Delta u) \text{ for } \Delta u = u - N/2, u = N/2+1, \dots, N-1$$

15

and the cosine C(u) and sine S(Δu) code vectors are the code vectors of the Fourier code matrix F.

20 The DFT (discrete Fourier transform) orthogonal codes are a complex basis for the complex N-dimensional CDMA code space  $C^N$  and consist of the DFT harmonic code vectors arranged in increasing order of frequency. Equations (4) are the definition of the DFT code vectors. The DFT definition (4) in equation (4) is widely  
25 known within the engineering and scientific communities. Even and odd components of the DFT code vectors (4) in equation (4) are the real cosine code vectors {C(u)} and the imaginary sine code vectors {S(u)} where even and odd are referenced to the midpoint of the code vectors. These cosine and sine code vectors  
30 in  $C^N$  are the extended set  $2N$  of the Fourier cosine and sine code vectors in  $R^N$ .

**40** DFT code vectors

$E$  = DFT  $N \times N$  orthogonal code matrix consisting of  
 5         $N$  rows of  $N$  chip code vectors  
       = [  $E(u)$  ] matrix of row vectors  $E(u)$   
       = [  $E(u,n)$  ] matrix of elements  $E(u,n)$   
 $E(u)$  = DFT code vector  $u$   
       = [  $E(u,0), E(u,1), \dots, E(u,N-1)$  ]  
 10        =  $1 \times N$  row vector of chips  $E(u,0), \dots, E(u,N-1)$   
 $E(u,n)$  = DFT code  $u$  chip  $n$   
       =  $e^{j2\pi un/N}$   
       =  $\cos(2\pi un/N) + j\sin(2\pi un/N)$   
       =  $N$  possible values on the unit circle

15

**41** Even and odd code vectors are the extended set of  
 Fourier even and odd code vectors in **39** equations (3\_)

$C(u)$  = Even code vectors for  $u=0,1,\dots,N-1$   
       = [  $1, \cos(2\pi u 1/N), \dots, \cos(2\pi u (N-1)/N)$  ]  
 20         $S(u)$  = Odd code vectors for  $u=0,1,\dots,N-1$   
       = [  $0, \sin(2\pi u 1/N), \dots, \sin(2\pi u (N-1)/N)$  ]  
 $E(u) = C(u) + j S(u)$  for  $u=0,1,\dots,N-1$

25

## 1. Hybrid Walsh Implementation Algorithm

Step 1 in the derivation of the implementation algorithm  
 30 for the Hybrid Walsh codes in this invention establishes the  
 correspondence of the even and odd Walsh codes with the even and  
 odd Fourier codes. Even and odd for these codes are with respect  
 to the midpoint of the row vectors similar to the definition for



the DFT vector codes **41** in equations **(4)**. Equations **(5)** identify the even and odd Walsh codes in the  $W$  basis in  $R^N$ . These even and odd Walsh codes can be placed in

5

Even and odd Walsh codes in  $R^N$  **(5)**

$$\begin{aligned} W_e(u) &= \text{Even Walsh code vector} \\ &= W(2u) \quad \text{for } u=0,1,\dots,N/2-1 \end{aligned}$$

$$\begin{aligned} W_o(u) &= \text{Odd Walsh code vectors} \\ 10 \quad &= W(2u-1) \quad \text{for } u=1,\dots,N/2 \end{aligned}$$

direct correspondence with the Fourier code vectors **39** in equations **(3)** using the DFT equations **(4)**. This correspondence  
15 is defined in equations **(6)** where the correspondence operator " $\sim$ " represents the even and odd correspondence between the Walsh and Fourier codes, and additionally represents the sequency~frequency correspondence.

20

Correspondence between Walsh and Fourier codes **(6)**

$$\begin{aligned} W(0) &\sim C(0) \\ W_e(u) &\sim C(u) \quad \text{for } u=1,\dots,N/2-1 \\ 25 \quad W_o(u) &\sim S(u) \quad \text{for } u=1,\dots,N/2-1 \\ W(N-1) &\sim C(N/2) \end{aligned}$$

Step 2 in the derivation of the implementation algorithm  
30 for the Hybrid Walsh codes derives the set of  $N$  complex DFT vector codes in  $C^N$  from the set of  $N$  real Fourier vector codes in  $R^N$ . This means that the set of  $2N$  cosine and sine code vectors in **41** in equations **(4)** for the DFT codes in  $C^N$  will be derived from the set of  $N$  cosine and sine code vectors in **39** in  
35 equations **(3)** for the Fourier codes in  $R^N$ . The first  $N/2+1$  code

vectors of the DFT basis can be written in terms of the Fourier code vectors in equations (7).

5 DFT code vectors  $0, 1, \dots, N/2$  derived from Fourier (7)

42 Fourier code vectors from 39 in equations (3) are

$$\begin{aligned} C(u) &= \text{Even code vectors for } u=0, 1, \dots, N/2 \\ &= [1, \cos(2\pi u_1/N), \dots, \cos(2\pi u(N-1)/N)] \end{aligned}$$

10 
$$\begin{aligned} S(u) &= \text{Odd code vectors for } u=1, 2, \dots, N/2-1 \\ &= [\sin(2\pi u_1/N), \dots, \sin(2\pi u(N-1)/N)] \end{aligned}$$

43 DFT code vectors in 41 of equations (4) are written as functions of the Fourier code vectors

15 
$$\begin{aligned} E(u) &= \text{DFT complex code vectors for } u=0, 1, \dots, N/2 \\ &= C(0) \quad \text{for } u=0 \\ &= C(u) + jS(u) \quad \text{for } u=1, \dots, N/2-1 \\ &= C(N/2) \quad \text{for } u=N/2 \end{aligned}$$

20

The remaining set of  $N/2+1, \dots, N-1$  DFT code vectors in  $C^N$  can be derived from the original set of Fourier code vectors by a correlation which establishes the mapping of the DFT codes onto the Fourier codes. We derive this mapping by correlating the

25 real and imaginary components of the DFT code vectors with the corresponding even and odd components of the Fourier code vectors. The correlation operation is defined in equations (8):

30 Correlation of DFT and Fourier code vectors (8)

$$\begin{aligned} \text{Corr}(\text{even}) &= C * \text{Real}\{E'\} \\ &= \text{Correlation matrix} \\ &= \text{Matrix product of } C \text{ and the real part} \\ &\quad \text{of } E \text{ conjugate transpose} \end{aligned}$$

35

$\text{Corr}(\text{odd}) = S \cdot \text{Imag}\{E'\}$   
 = Correlation matrix  
 = Matrix product of S and the imaginary  
 part of E conjugate transpose

5

where "\*" is a matrix multiply operation. The correlation peaks  
 of these correlation matrices are plotted in FIG.5 for N=32 for  
 the real cosine and the odd sine Fourier code vectors. Plotted  
 10 are the correlation peaks of the 2N DFT cosine and sine codes  
 against the N Fourier cosine and sine codes which range from -15  
 to +16 where the negative indices of the codes represent a  
 negative correlation value. These correlation curves prove that  
 the remaining  $N/2+1, \dots, N-1$  code vectors of the DFT are derived  
 15 from the Fourier code vectors by equations (9)

DFT code vectors  $N/2+1, \dots, N-1$  derived from Fourier (9)

20

$E(u) = C(N/2 - \Delta u) - jS(N/2 - \Delta u)$   
 for  $u = N/2 + \Delta u$   
 $\Delta u = 1, \dots, N/2-1$

25

This construction of the remaining DFT basis in equations (9) is  
 an application of the DFT spectral foldover property which  
 observes the DFT harmonic vectors for frequencies  $f_{NT} = N/2 + \Delta u$   
 above the Nyquist sampling rate  $f_{NT} = N/2$  simply foldover such  
 30 that the DFT harmonic vector for  $f_{NT} = N/2 + \Delta u$  is the DFT basis  
 vector for  $f_{NT} = N/2 - \Delta u$  to within a fixed sign and fixed phase  
 angle of rotation.

Step 3 is the final step in the derivation of the  
 35 implementation algorithm for the Hybrid Walsh codes and derives

the HybridWalsh code vectors from the real Walsh code vectors by using the DFT derivation in equations (7) and (9), by using the correspondences between the real Walsh and Fourier in equations (6), and by using the fundamental correspondence between the Hybrid Walsh and the complex DFT given in equation (10). We start by constructing the Hybrid Walsh

#### Correspondence between Hybrid Walsh and DFT (10)

10

$\tilde{W} \sim E$  NxN complex DFT orthogonal code matrix

where  $W =$  NxN Hybrid Walsh orthogonal code matrix

$=$  N rows of N chip code vectors

$= [ \tilde{W}(u) ]$  matrix of row vectors  $\tilde{W}(u)$

15

$= [ \tilde{W}(u,n) ]$  matrix of elements  $\tilde{W}(u,n)$

$\tilde{W}(u) =$  Hybrid Walsh code vector u

$= [ \tilde{W}(u,0), \tilde{W}(u,1), \dots, \tilde{W}(u,N-1) ]$

$\tilde{W} = +/-1 +/- j$  possible value

20

dc (0 frequency and 0 sequency) code vector  $\tilde{W}(0)$ . We use equation  $E(0)=C(0)$  in 43 in equations (7), the correspondence in equations (6), and observe that the dc Hybrid Walsh vector has both real and imaginary components in the  $\tilde{W}$  domain, to derive the dc Hybrid Walsh code vector:

25

$$\tilde{W}(0) = W(0) + jW(0) \quad \text{for } u=0 \quad (11)$$

30

For Hybrid Walsh code vectors  $\tilde{W}(u)$ ,  $u=1,2,\dots,N/2-1$ , we apply the correspondences in equations (10) between the Hybrid Walsh and

DFT bases and the correspondence in equation (6) to the DFT equations 43 in equations (7):

$$\begin{aligned} \tilde{W}(u) &= W_e(u) + jW_o(u) & \text{for } u=1,2,\dots,N/2-1 \\ &= W(2u) + jW(2u-1) & \text{for } u=1,2,\dots,N/2-1 \end{aligned} \quad (12)$$

For Hybrid Walsh code vector  $\tilde{W}(N/2)$  we use the equation  
 10  $E(N/2)=C(N/2)$  43 in equations (7) and the same rationale used  
 to derive equation (11), to yield the equation for  $\tilde{W}(N/2)$ .

$$\tilde{W}(N/2) = W(N-1) + jW(N-1) \quad \text{for } u=N/2 \quad (13)$$

15

For Hybrid Walsh code vectors  $\tilde{W}(N/2+\Delta u)$ ,  $\Delta u=1,2,\dots,N/2-1$  we  
 apply the correspondences between the Hybrid Walsh and DFT bases  
 20 to the spectral foldover equation  $E(N/2+\Delta u)=C(N/2-\Delta u)-jS(N/2-\Delta u)$   
 in equation (9) with the changes in indexing required to account  
 for the  $W$  indexing in equations (5). The equation is

$$\begin{aligned} \tilde{W}(N/2+\Delta u) &= W(N-1-\Delta e u) + W(N-1-\Delta o u) & \text{for } u=N/2+1,\dots,N-1 \\ &= W(N-1-2\Delta u) + jW(N-2\Delta u) & \text{for } u=N/2+1,\dots,N-1 \end{aligned} \quad (14)$$

using the notation  $\Delta e i=2\Delta i$ ,  $\Delta o i=2\Delta i-1$ . These Hybrid Walsh code  
 30 vectors in equations (11), (12), (13), (14) are the equations of  
 definition for the Hybrid Walsh code vectors.

An equivalent way to derive the Hybrid Walsh code vectors in  $C^N$  from the real Walsh basis in  $R^{2N}$  is to use a sampling technique which is a known method for deriving a complex DFT basis in  $C^N$  from a Fourier real basis in  $R^N$  as demonstrated in  
5 FIG. 5.

FIG. 6B and 6C summarize the Hybrid Walsh implementation algorithms derived in Steps 1,2,3 for implementation as lexicographic reordering permutations of the real Walsh code  
10 vectors and lexicographic reordering permutations of the even and odd Walsh code vectors, with the reordering lexicographically arranged with increasing sequency in agreement with the correspondence "sequency ~ frequency" for "Hybrid Walsh ~ DFT".

FIG. 6B summarizes equations (5), (11), (12), (13), (14) which  
15 define the real (inphase) 168 and imaginary (quadrature) 169 reordering permutations for implementation of the Hybrid Walsh. The inphase reordering permutation 168 in FIG. 6B is implemented as an address change of the row vectors in  $W$  to correspond to the  
20 row vectors in  $\underline{W}_R$  in lexicographic ordering with increasing sequency 167. Likewise, the quadrature reordering permutation 169 is implemented as an address change of the row vectors in  $W$  to correspond to the row vectors in  $\underline{W}_I$  in lexicographic ordering with increasing sequency 167. These reordering permutations  
25 define the Hybrid Walsh  $\tilde{W} = W_R + j W_I$ .

FIG. 6C reorganizes the implementation algorithm for the Hybrid Walsh in FIG. 6B as lexicographic reordering permutations of the even and odd real Walsh code vectors defined in equations  
30 (5), (11), (12), (13), (14). The real (inphase) and quadrature reordering permutations 171, 172 are address changes of the even, odd real Walsh vectors with increasing sequency 170. These reordering permutations define the Hybrid Walsh  $\tilde{W} = W_R + j W_I$ .

## 2. Hybrid Walsh Implementation

5

Transmitter equations (15) describe a representative Hybrid Walsh CDMA encoding implementation algorithm for the transmitter in FIG. 1A upon replacing the real Walsh with the Hybrid Walsh, and for the cellular network in FIG. 1B and transmitter FIG. 6D, and for the encoding implementation in FIG. 6A. It is assumed that there are N Hybrid Walsh code vectors  $\tilde{W}(u)$  44 each of length N chips similar to the definitions for the real Walsh code vectors 1 in equations (1). The code vector is presented by a 1xN N-chip row vector  $\tilde{W}(u) = [\tilde{W}(u,0), \dots, \tilde{W}(u,N-1)]$  where  $\tilde{W}(u,n)$  is chip n of code u. The code vectors are the row vectors of the Hybrid Walsh matrix  $\tilde{W}$ . Hybrid Walsh code chip n of code vector u has the possible values  $\tilde{W}(u,n) = +/-1 +/-j$ . Each user is assigned a unique Walsh code which allows the code vectors to be designated by the user symbols  $u=0,1,\dots,N-1$  for N Hybrid Walsh codes. The Hybrid Walsh code vectors  $\tilde{W}(u)$  derived in equations (11), (12), (13), (14) and equivalently in FIG. 6B, 6C are summarized 44 in terms of their real and imaginary component code vectors  $\tilde{W}(u) = W_R(u) + jW_I(u)$  where  $W_R(u)$  and  $W_I(u)$  are respectively the real and imaginary component code vectors. As per the derivation of  $\tilde{W}(u)$  the sets of real axis code vectors  $\{W_R(u)\}$  and the imaginary axis code vectors  $\{W_I(u)\}$  both consist of the real Walsh code vectors in  $R^N$  with the ordering modified to ensure that the definition of the Hybrid Walsh vectors satisfies equations (11), (12), (13), (14).

**44** Hybrid Walsh codes use the definitions for the real Walsh codes in 1 equations (1) and the definitions of the Hybrid Walsh codes in equations (11), (12), (13), (14) and in FIG. 6B, 6C. We find

$$\begin{aligned}\tilde{W} &= \text{Hybrid Walsh } N \times N \text{ orthogonal code matrix} \\ &\text{consisting of } N \text{ rows of } N \text{ chip code vectors} \\ &= [ \tilde{W}(u) ] \text{ matrix of row vectors } \tilde{W}(u) \\ &= [ \tilde{W}(u,n) ] \text{ matrix of elements } \tilde{W}(u,n)\end{aligned}$$

$$\begin{aligned}\tilde{W}(u) &= \text{Hybrid Walsh code vector } u \\ &= W_R(u) + jW_I(u) \quad \text{for } u=0,1,\dots,N-1\end{aligned}$$

where

$$\begin{aligned}W_R(u) &= \text{Real}\{ \tilde{W}(u) \} \\ &= W(0) \quad \text{for } u=0 \\ &= W(2u) \quad \text{for } u=1,2,\dots,N/2-1 \\ &= W(N-1) \quad \text{for } u=N/2 \\ &= W(2N-2u-1) \quad \text{for } u=N/2+1,\dots,N-1\end{aligned}$$

$$\begin{aligned}W_I(u) &= \text{Imag}\{ \tilde{W}(u) \} \\ &= W(0) \quad \text{for } u=0 \\ &= W(2u-1) \quad \text{for } u=1,2,\dots,N/2-1 \\ &= W(N-1) \quad \text{for } u=N/2 \\ &= W(2N-2u) \quad \text{for } u=N/2+1,\dots,N-1\end{aligned}$$

$$\begin{aligned}\tilde{W}(u,n) &= \text{Hybrid Walsh code } u \text{ chip } n \\ &= +/-1 +/-j \text{ possible values}\end{aligned}$$

**45** Data symbols

$$\begin{aligned}Z(u) &= \text{Complex data symbol for user } u \\ &= R(u) + jI(u)\end{aligned}$$



**46** Hybrid Walsh encoded data

$$\begin{aligned}
 Z(u,n) &= Z(u) \tilde{W}(u,n) \\
 &= Z(u) [\text{sign}\{W_R(u,n)\} + j\text{sign}\{W_I(u,n)\}] \\
 &= [R(u)\text{sign}\{W_R(u,n)\} - I(u)\text{sign}\{W_I(u,n)\}] \\
 &\quad + j[R(u)\text{sign}\{W_I(u,n)\} + I(u,n)\text{sign}\{W_R(u,n)\}]
 \end{aligned}$$

**47** PN scrambling

$$\begin{aligned}
 P_2(n) &= \text{Chip } n \text{ of the long PN code} \\
 P_R(n) &= \text{Chip } n \text{ of the short PN code for the real axis} \\
 P_I(n) &= \text{Chip } n \text{ of the short PN code for the imaginary axis} \\
 Z(n) &= \text{PN scrambled Hybrid Walsh encoded data chips after summing over the users} \\
 &= \sum_u Z(u,n) P_2(n) [P_R(n) + j P_I(n)] \\
 &= \sum_u Z(u,n) \text{sign}\{P_2(n)\} [\text{sign}\{P_R(n)\} + j \text{sign}\{P_I(n)\}] \\
 &= \text{Hybrid Walsh CDMA encoded chips}
 \end{aligned}$$

User data symbols **45** are the set of complex symbols  $\{Z(u), u=0,1,\dots,N-1\}$ . These data symbols are encoded by the Hybrid Walsh CDMA codes **46**. Each of the user symbols  $Z(u)$  is assigned a unique Hybrid Walsh code  $\tilde{W}(u)=W_R(u)+jW_I(u)$ . Hybrid Walsh encoding of each user data symbol generates an N-chip sequence with each chip in the sequence consisting of the user data symbol with the complex sign of the corresponding Hybrid Walsh code chip, which means each encoded chip = [Data symbol  $Z(u)$ ] x [Sign of  $W_R(u)$  + j sign of  $W_I(u)$ ].

The Hybrid Walsh encoded data symbols are summed and encoded with PN scrambling codes **47**. These long and short PN codes are defined **4** in equations **(1)**. Each Hybrid Walsh encoded data chip  $Z(u,n)$  **46** is summed over the set of users  $u=0,1,\dots,N-$

1 and PN encoded to yield the Hybrid Walsh CDMA chips  $Z(n) = \sum_u Z(u,n) P_2(n) [P_R(n) + j P_I(n)]$  **47**.

Although not considered in this example, it is possible to use combinations of both complex and real data symbols similar to the approach for real Walsh CDMA encoding in equations **(1)** since the Hybrid Walsh code vectors are a reordering of the real Walsh code vectors along the real axis and a reordering of the real Walsh code vectors along the imaginary axis.

Receiver equations **(16)** describe a representative Hybrid Walsh CDMA decoding implementation algorithm for the receiver in FIG. **3A** upon replacing the real Walsh with the Hybrid Walsh, and for the cellular network in FIG. **1B** and receiver FIG. **7B**, and for the decoding implementation in FIG. **7A**. The receiver front end **48** provides estimates  $\{\hat{Z}(n)\}$  of the transmitted Hybrid Walsh CDMA encoded chips  $\{Z(n)\}$  for the complex data symbols  $\{Z(u)\}$ . Orthogonality property **49** is expressed as a matrix product of the Hybrid Walsh code chips or equivalently as a matrix product of the Hybrid Walsh code chip numerical signs of the real and imaginary components. Decoding algorithms **51** perform the inverse of the signal processing for the encoding in equations **(15)** to recover estimates  $\{\hat{Z}(u)\}$  of the transmitter user symbols  $\{Z(n)\}$  for the complex data symbols  $\{Z(u)\}$ .

Hybrid Walsh CDMA decoding for receiver **(16)**

**48** Receiver front end in FIG. **3A** provides estimates  $\{\hat{Z}(n)\}$  **28** of the encoded transmitter chip symbols  $\{Z(n)\}$  **47** in equations **(15)**.

**49** Orthogonality property of Hybrid Walsh  $N \times N$  matrix  $\tilde{W}$

$$\sum_n \tilde{W}(\hat{u}, n) \tilde{W}'(n, u) =$$

$$\sum_n [\text{sign}\{W_R(\hat{u}, n)\} + j \text{sign}\{W_I(\hat{u}, n)\}] [\text{sign}\{W_R(n, u) - j \text{sign}\{W_I(n, u)\}\}]$$

$$= 2N \delta(\hat{u}, u)$$

5 where  $\delta(\hat{u}, u)$  = Delta function of  $\hat{u}$  and  $u$

$$= 1 \quad \text{for } \hat{u} = u$$

$$= 0 \quad \text{otherwise}$$

$$\tilde{W}' = \text{conjugate transpose of } \tilde{W}$$

10 **50** PN decoding property

$$P(n)P(n) = \text{sign}\{P(n)\} \text{sign}\{P(n)\}$$

$$= 1$$

for  $P = P_2, P_R, P_I$

15 **51** Decoding algorithm

$$\hat{Z}(u) =$$

$$2^{-1}N^{-1} \sum_n \hat{Z}(n) \text{sign}\{P_2(n)\} [\text{sign}\{P_R(n)\} - j \text{sign}\{P_I(n)\}]^*$$

$$[\text{sign}\{W_R(n, u)\} - j \text{sign}\{W_I(n, u)\}]$$

= Receiver estimate of the transmitted data symbol

$Z(u)$  **45** in equations **(15)**

20 where "\*" denotes a multiply

Although not considered in this example, it is possible to use combinations of both complex and real data symbols similar to the approach for real Walsh CDMA decoding in FIG. 4 since the Hybrid Walsh code vectors are the real Walsh code vectors along the real axis and a reordering of the real Walsh code vectors along the imaginary axis.

FIG. **6A** Hybrid Walsh CDMA encoding is a representative implementation of the Hybrid Walsh CDMA encoding which will replace the current real Walsh encoding **13** in FIG. **1A** and in the cellular network transmitter implementation **120,121** in FIG. **1C**, and is defined in equations (15). Inputs are the user data symbols  $\{Z(u)\}$  **52**. Encoding of each user by the corresponding Hybrid Walsh code is described in **53** by the implementation of transferring the sign  $\pm 1/\pm j$  of each Hybrid Walsh code chip to the user data symbol followed by a 1-to-N expander  $1 \uparrow N$  of each data symbol into an N chip sequence using the sign transfer of the Hybrid Walsh chips. The sign-expander operation **53** generates the N-chip sequence

$$Z(u,n) = Z(u) [\text{sign}\{W_R(u,n)\} + j \text{sign}\{W_I(u,n)\}] = Z(u) [W_R(u,n) + j W_I(u,n)]$$

for  $n=0,1,\dots,N-1$  for each user  $u=0,1,\dots,N-1$ . This Hybrid Walsh encoding serves to spread each user data symbol into an orthogonally encoded chip sequence which is spread over the CDMA communications frequency band. The Hybrid Walsh encoded chip sequences for each of the user data symbols are summed over the users **54** followed by PN encoding with the scrambling sequence  $P_2(n) [P_R(n) - j P_I(n)]$  **55**. PN encoding is implemented by transferring the sign of each PN chip to the summed chip of the Hybrid Walsh encoded data symbols. Output is the stream of complex CDMA encoded chips  $\{Z(n)\}$  **56**.

FIG. **6D** is the upgrade to the cellular network transmit CDMA encoding in FIG. **1C** using the Hybrid Walsh channelization codes in place of the real Walsh codes. FIG. **6D** depicts a representative embodiment of the transmitter signal processing for the forward and reverse CDMA links **106** in FIG. **1B** between the base station and the user for CDMA2000 and W-CDMA. Similar to FIG. **1C** the data inputs are the inphase data symbols  $R$  **173** and quadrature data symbols  $I$  **174**. Inphase **175** Hybrid Walsh codes  $\underline{W}_I$  are implemented in FIG. **6B 167,168** and equivalently in FIG. **6C**

170,171. Quadrature 176 Hybrid Walsh codes  $\underline{W}_I$  are implemented in FIG. 6B 167,169 and equivalently in FIG. 6C 170,172. A complex multiply 177 encodes the data symbols with the Hybrid Walsh  $\tilde{W}$  codes in the encoder using the inphase (real)  $\underline{W}_R$  and quadrature (imaginary)  $\underline{W}_I$  code components of  $\tilde{W} = \underline{W}_R + j\underline{W}_I$  to generate a rate  $R=N$  set of Hybrid Walsh encoded data chips for each inphase and quadrature data symbol. Following the Hybrid Walsh encoding the transmit signal processing in 178-to-189 is identical to the corresponding transmit signal processing in 122-to-133 in FIG. 1C.

FIG. 6D depicts an embodiment of the upgrade to the current CDMA transmitter art using the Hybrid Walsh codes in place of the real Walsh codes and with current art signal processing changes this figure is representative of the use of Hybrid Walsh codes in place of the real Walsh codes for other current art CDMA receiver embodiments of this invention disclosure. Other embodiments of the CDMA transmitter include changes in the ordering of the signal processing, single channel versus multi-channel Hybrid Walsh encoding, summation or combining of the Hybrid Walsh channels by summation over like chip symbols, analog versus digital signal representation, baseband versus IF frequency CDMA processing, the order and placement in the signal processing thread of the  $\Sigma$ , LPF, and D/A signal processing operations, and the up-conversion processing. The order of the rate  $R=1$  PN code multiplies in FIG. 6D can be changed since the covering operations implemented by the multiplies are linear in phase, which means the short code complex multiply 180,181,182 in FIG. 6D can occur prior to the long code multiply 178,179 and moreover the long code can be complex with the real multiply 179 replaced by the equivalent complex multiply 182.

Although not considered in these examples, it is possible to use combinations of both complex and real data symbols similar

to the approach for real Walsh CDMA encoding in FIG. 2 since the Hybrid Walsh code vectors are the reordered real Walsh code vectors along the real axis and a reordering of the real Walsh code vectors along the imaginary axis.

5

It should be obvious to anyone skilled in the communications art that the example implementations in FIG. 6A, 6D clearly define the fundamental CDMA signal processing relevant to this invention disclosure and it is obvious that these examples are representative of the other possible signal processing approaches.

FIG. 7A Hybrid Walsh CDMA decoding is a representative implementation of CDMA complex channelization decoding which will replace the current real Walsh decoding 27 in FIG. 3A, and is defined in equations (16). Inputs are the received estimates of the complex CDMA encoded chips  $\{\hat{Z}(n)\}$  57. The PN codes are stripped off from these chips 58 by changing the sign of each chip according to the numerical sign of the real and imaginary components of the complex conjugate of the PN code as per the decoding algorithm 51 in equations (16).

The Hybrid Walsh channelization coding is removed by a pulse compression operation consisting of multiplying each received chip by the numerical sign of the corresponding Hybrid Walsh chip for the user and summing the products over the N Walsh chips 59 to recover estimates  $\{\hat{Z}(u)\}$  of the user complex data symbols  $\{Z(u)\}$ .

FIG. 7B is the upgrade to the cellular network receive CDMA decoding in FIG. 3B using the Hybrid Walsh complex channelization codes in place of the real Walsh codes. FIG. 7B depicts a representative embodiment of the receiver signal processing for the forward and reverse CDMA links 106 in FIG. 1B

between the base station and the user for CDMA2000 and W-CDMA that implements the CDMA decoding for the discovering by the long code and the short complex codes followed by the Hybrid Walsh decoding to recover estimates of the transmitted inphase (real) data symbols  $R$  173 and quadrature (imaginary) data symbols  $I$  174 in FIG. 6D. Depicted are the principal signal processing that is relevant to this invention disclosure. Similar to FIG. 3B the signal input  $\hat{v}(t)$  190 is the received estimate of the transmitted CDMA signal  $v(t)$  189 in FIG. 6D. The receive signal recovery in 191-to-201 is identical to the corresponding receive signal processing in 135-to-145 in FIG. 3B. The discovered chip symbols are rate  $R=1/N$  decoded by the Hybrid Walsh complex decoder 204 using the complex conjugate of the Hybrid Walsh code structured as the inphase Hybrid Walsh code  $\underline{W}_R$  202 and the negative of the quadrature Hybrid Walsh code  $(-)\underline{W}_I$  203 to implement the complex conjugate of the Hybrid Walsh code in the complex multiply and decoding operations. Decoded output symbols are the inphase data symbol estimates  $\hat{R}$  205 and the quadrature data symbol estimates  $\hat{I}$  206.

FIG. 7B depicts an embodiment of the upgrade to the current CDMA receiver art using the Hybrid Walsh code in place of the real Walsh code and with current art signal processing changes this figure is representative of the use of Hybrid Walsh codes in place of the real Walsh codes for other current art CDMA receiver embodiments of this invention disclosure. Other embodiments of the CDMA receiver include changes in the ordering of the signal processing, analog versus digital signal representation, down-conversion processing, baseband versus IF frequency CDMA processing, the order and placement in the signal processing thread of the  $\Sigma$ , LPF, and A/D signal processing operations, and single channel versus multi-channel Hybrid Walsh decoding, The order of the rate  $R=1$  PN code multiplies in FIG. 7B which perform the code discovering can be changed since the covering

operations implemented by the multiplies are linear in phase,  
which means the short code complex multiply **197,198,199** can  
occur after to the long code multiply **200,201** and moreover the  
long code can be complex with the real multiply **201** replaced by  
5 the equivalent complex multiply **199**.

Although not considered in these examples, it is possible  
to use combinations of both complex and real data symbols similar  
to the approach for real Walsh CDMA decoding in FIG. **4** since the  
10 Hybrid Walsh code vectors are the real Walsh code vectors along  
the real axis and a reordering of the real Walsh code vectors  
along the imaginary axis.

It should be obvious to anyone skilled in the  
15 communications art that these example implementations in FIG.  
**7A,7B** clearly define the fundamental CDMA signal processing  
relevant to this invention disclosure and it is obvious that  
this example is representative of the other possible signal  
processing approaches.

20 For cellular applications the transmitter description  
describes the transmission signal processing applicable to this  
invention for both the hub and user terminals, and the receiver  
describes the corresponding receiving signal processing for the  
25 hub and user terminals for applicability to this invention.

30



### 3. Generalized Hybrid Walsh Codes using Tensor Product, Direct Sum, and Functional Combining

5

Generalized Hybrid Walsh codes enable the power of 2 code lengths  $N=2^M$  where  $M$  is an integer for Hybrid Walsh to be modified to allow the code length  $N$  to be a product of powers of primes **60** in equations **(17)** or a sum of powers of primes **61** in equations **(17)**, at the implementation cost of introducing multiply operations into the CDMA encoding and decoding. In the previous disclosure of this invention we used  $N$  equal to a power of 2 which means  $N=2^M$  corresponding to prime  $p_0 = 2$  and  $M=m_0$ . This restriction was made for convenience in explaining the construction of the Hybrid Walsh and is not required since it is well known that Hadamard matrices exist for non-integer powers of 2 and, therefore, Hybrid Walsh matrices exist for non-integer powers of 2.

20

Length  $N$  of generalized Hybrid Walsh orthogonal codes **(17)**

**60** Tensor product code construction

$$\begin{aligned} N &= \prod_k p_k^{m_k} \\ &= \prod_k N_k \end{aligned}$$

25

where

$p_k$  = prime number indexed by  $k$  starting with  $k=0$

$m_k$  = order of the prime number  $p_k$

$N_k$  = Length of code for the prime  $p_k$

30

$$= p_k^{m_k}$$

## 61 Direct sum code construction

$$\begin{aligned} N &= \sum_k p_k^{m_k} \\ &= \sum_k N_k \end{aligned}$$

5        Add-only arithmetic operations are required for encoding  
and decoding both real Walsh and Hybrid Walsh CDMA codes since  
the real Walsh values are  $\pm 1$  and the Hybrid Walsh values are  
 $\{\pm 1, \pm j\}$  or equivalently are  $\{1, j, -1, -j\}$  under a  $-90$  degree  
rotation and normalization which means the only operations are  
10    sign transfer and adds plus subtracts or add-only.    Multiply  
operations are more complex to implement than add operations.  
However, the advantages of having greater flexibility in  
choosing the orthogonal CDMA code lengths  $N$  using equations (17)  
can offset the expense of multiply operations for particular  
15    applications. Accordingly, this invention includes the concept  
of generalized Hybrid Walsh orthogonal CDMA codes with the  
flexibility to meet these needs. This extended class of Hybrid  
Walsh codes supplement the Hybrid Walsh codes by combining with  
Hadamard (or real Walsh), DFT, and other orthogonal codes as well  
20    as with PN by relaxing the orthogonality property to quasi-  
orthogonality.

Generalized Hybrid Walsh orthogonal CDMA codes can be  
constructed as demonstrated in 64 and 65 in equations (18)  
25    for the tensor product, and in 66 in equations (18) for the  
direct sum, and in 67 for functional combining. Code matrices  
considered for orthogonal CDMA codes are 62 in equations (18)  
for the construction of the generalized Hybrid Walsh are the DFT  
E and Hadamard H, in addition to the Hybrid Walsh  $\tilde{W}$ . The  
30    algorithms and examples for the construction start with the  
definitions 63 of the  $N \times N$  orthogonal code matrices  $\tilde{W}_N, E_N, H_N$   
for  $\tilde{W}, E, H$  respectively, examples for low orders  $N=2, 4$ , and the

equivalence of  $E_4$  and  $\tilde{W}_4$  after the  $\tilde{W}_4$  is rotated through the angle  $-90$  degrees and rescaled. The CDMA current and developing standards use the prime 2 which generates a code length  $N=2^M$  where  $M=\text{integer}$ . For applications requiring greater flexibility in code length  $N$ , additional primes can be used using the tensor construction. We illustrate this in **65** with the addition of prime=3. The use of prime=3 in addition to the prime=2 in the range of  $N=8$  to 64 is observed to increase the number of  $N$  choices from 4 to 9 at a modest cost penalty of using multiples of the angle increment 30 degrees for prime=3 in addition to the angle increment 90 degrees for prime=2. As noted in **65** there are several choices in the ordering of the tensor product construction and 2 of these choices are used in the construction. In general, different orderings of the tensor product yield different sets of orthogonal codes.

Direct sum construction provides greater flexibility in the choice of  $N$  without necessarily introducing a multiply penalty. However, the addition of the zero matrix in the construction is generally not desirable for CDMA communications. A functional combining in **67** in equation (18) removes these zero matrices at the cost of relaxing the orthogonality property to quasi-orthogonality.

25

Construction of generalized Hybrid Walsh orthogonal  
and quasi-orthogonal codes **(18)**

## **62** Code matrices for orthogonal codes

30  $\tilde{W}_N$  =  $N \times N$  Hybrid Walsh orthogonal code matrix  
 $E_N$  =  $N \times N$  DFT orthogonal code matrix  
 $H_N$  =  $N \times N$  Hadamard orthogonal code matrix

### 63 Low-order orthogonal code definitions and equivalences

$$2 \times 2 \quad H_2 = \begin{bmatrix} 1 & 1 \\ 1 & -1 \end{bmatrix}$$

$$5 \quad = E_2$$

$$= (e^{-j\pi/4} / \sqrt{2}) * \tilde{W}_2$$

$$10 \quad 3 \times 3 \quad E_3 = \begin{bmatrix} 1 & 1 & 1 \\ 1 & e^{j2\pi/3} & e^{j2\pi/3} \\ 1 & e^{j2\pi/3} & e^{j2\pi/3} \end{bmatrix}$$

$$15 \quad 4 \times 4 \quad H_4 = \begin{bmatrix} 1 & 1 & 1 & 1 \\ 1 & -1 & 1 & -1 \\ 1 & 1 & -1 & -1 \\ 1 & -1 & -1 & 1 \end{bmatrix}$$

$$20 \quad \tilde{W}_4 = \begin{bmatrix} 1+j & 1+j & 1+j & 1+j \\ 1+j & -1+j & -1-j & 1-j \\ 1+j & -1-j & 1+j & -1-j \\ 1+j & 1-j & -1-j & -1+j \end{bmatrix}$$

$$25 \quad E_4 = \begin{bmatrix} 1 & 1 & 1 & 1 \\ 1 & j & -1 & -j \\ 1 & -1 & 1 & -1 \\ 1 & -j & -1 & j \end{bmatrix}$$

$$30 \quad = (e^{-j\pi/4} / \sqrt{2}) \tilde{W}_4$$

**64** Tensor product construction for  $N = \prod_k N_k$

Code matrix  $C_N = N \times N$  generalized Hybrid  
Walsh CDMA orthogonal code matrix using the  
tensor product construction of  $C_N$

$$C_N = C_0 \prod_{k>0} \otimes C_{N_k}$$

Tensor product definition

$A = N_a \times N_a$  orthogonal code matrix

$B = N_b \times N_b$  orthogonal code matrix

$A \otimes B =$  Tensor product of matrix A and matrix B

$= N_a N_b \times N_a N_b$  orthogonal code matrix consisting  
of the elements  $[a_{ik}]$  of matrix A multiplied  
by the matrix B

$$= [a_{ik} B]$$

**65** Generalized Hybrid Walsh orthogonal code matrix  
tensor product construction examples for primes  
 $p=2,3$  and the range of sizes  $8 \leq N \leq 64$

$$8 \times 8 \quad C_8 = \tilde{W}_8$$

$$12 \times 12 \quad C_{12} = \tilde{W}_4 \otimes E_3$$

$$C_{12} = E_3 \otimes \tilde{W}_4$$

$$16 \times 16 \quad C_{16} = \tilde{W}_{16}$$

$$18 \times 18 \quad C_{18} = \tilde{W}_2 \otimes E_3 \otimes E_3$$

$$C_{18} = E_3 \otimes E_3 \otimes \tilde{W}_2$$

$$\begin{aligned} 24 \times 24 \quad C_{24} &= \tilde{W}_8 \otimes E_3 \\ C_{24} &= E_3 \otimes \tilde{W}_8 \end{aligned}$$

$$32 \times 32 \quad C_{32} = \tilde{W}_{32}$$

$$\begin{aligned} 36 \times 36 \quad C_{36} &= \tilde{W}_4 \otimes \tilde{W}_3 \otimes \tilde{W}_3 \\ C_{36} &= \tilde{W}_3 \otimes \tilde{W}_3 \otimes \tilde{W}_4 \end{aligned}$$

$$\begin{aligned} 48 \times 48 \quad C_{48} &= \tilde{W}_{16} \otimes \tilde{W}_3 \\ C_{48} &= \tilde{W}_3 \otimes \tilde{W}_{16} \end{aligned}$$

$$64 \times 64 \quad C_{64} = \tilde{W}_{64}$$

## 66 Generalized Hybrid Walsh orthogonal code

matrices using direct sum construction for  $N = \sum_k N_k$

Code matrix  $C_N = N \times N$  generalized Hybrid Walsh orthogonal Walsh CDMA code matrix with the direct sum construction of  $C_N$

$$C_N = C_0 \prod_{k>0} \oplus C_{N_k}$$

Direct sum definition

A =  $N_a \times N_a$  orthogonal code matrix

B =  $N_b \times N_b$  orthogonal code matrix

$A \oplus B$  = Direct sum of matrix A and matrix B

5 =  $N_a + N_b \times N_a + N_b$  orthogonal code matrix

$$= \begin{bmatrix} A & O_{N_a \times N_b} \\ O_{N_b \times N_a} & B \end{bmatrix}$$

10

where  $O_{N_1 \times N_2} = N_1 \times N_2$  zero matrix

**67** Generalized Hybrid Walsh quasi-orthogonal code

15 matrices using functional combining with

direct sum construction for  $N = \sum_k N_k$

Code matrix  $C_N = N \times N$  generalized Hybrid Walsh  
quasi-orthogonal Walsh CDMA code matrix using

20 functional combining with direct sum construction of  $C_N$

$$C_N = f( C_0 \prod_{k>0} \oplus C_{N_k} , C_P )$$

25

wherein

$f(A, b)$  = functional combining operator of A, B

= the element-by-element covering of

A with B for the elements of  $A \neq 0$ ,

= the element-by-element sum of A and

30

B for the elements of  $A = 0$

$C_p$  = NxN pseudo-orthogonal complex code matrix  
whose row code vectors are independent  
strips of PN codes for the real and  
imaginary components

5

It should be obvious to anyone skilled in the communications art that these example implementations of the generalized Hybrid Walsh in equations (18) clearly define the fundamental CDMA signal processing relevant to this invention disclosure and it is obvious that this example is representative of the other possible signal processing approaches. For example, the tensor product matrices  $E_N$  and  $H_N$  can be replaced by functionals.

15 For cellular applications the transmitter description which includes equations (18) describes the transmission signal processing applicable to this invention for both the hub and user terminals in FIG. 1B, and the receiver corresponding to the decoding of equations (18) describes the corresponding receiving  
20 signal processing for the hub and user terminals in FIG. 1B for applicability to this invention.

It is well known that fast and efficient encoding and decoding algorithms exist for the real Walsh CDMA codes. It is  
25 obvious that with suitable modifications these algorithms can be used to develop fast and efficient encoding and decoding algorithms for the Hybrid Walsh CDMA codes since these complex codes have real and imaginary code vectors which are from the same set of real Walsh CDMA codes.

30

It is well known that the tensor product construction involving DFT, H, W orthogonal code vectors have efficient encoding and decoding algorithms. It is obvious that with suitable modifications these algorithms can be used to develop  
35 fast and efficient encoding and decoding algorithms for the



tensor products of DFT, H. W,  $\tilde{W}$  CDMA codes since Hybrid Walsh codes have real and imaginary code vectors which are from the same set of real Walsh CDMA codes. It is obvious that fast and efficient encoding and decoding algorithms exist for direct sum  
5 construction and functional combining.

Preferred embodiments in the previous description is provided to enable any person skilled in the art to make or use the present invention. The various modifications to these  
10 embodiments will be readily apparent to those skilled in the art, and the generic principles defined herein may be applied to other embodiments without the use of the inventive faculty. Thus, the present invention is not intended to be limited to the embodiments shown herein but is not to be accorded the wider  
15 scope consistent with the principles and novel features disclosed herein.